A Simplified Two-Phase Flow Model Using a Quasi-Equilibrium Momentum Balance

Ulf Jakob F. Aarsnes[a,1,*], Adrian Ambrus[b], Florent Di Meglio[c], Ali Karimi Vajargah[d], Ole Morten Aamo[a], Eric van Oort[d]

[a]*Department of Engineering Cybernetics, NTNU, Trondheim, Norway*
[b]*Department of Mechanical Engineering, University of Texas at Austin*
[c]*Centre Automatique et Systmes, MINES ParisTech*
[d]*Department of Petroleum and Geosystems Engineering, University of Texas at Austin*

Abstract

We propose a simple model of two-phase gas-liquid flow by imposing a quasi-equilibrium on the mixture momentum balance of the classical transient drift-flux model. This reduces the model to a single hyperbolic PDE, describing the void wave, coupled with two static relations giving the void wave velocity from the now static momentum balance. Exploiting this, the new model uses a single distributed state, the void fraction, and with a suggested approximation of the two remaining static relations, all closure relations are given explicitly in, or as quadrature of functions of, the void fraction and exogenous variables. This makes model implementation, simulation and analysis very fast, simple and robust. Consequently, the proposed model is well-suited for model-based control and estimation applications concerning two-phase gas-liquid flow.

Keywords: Two-phase flow, Drilling, Well control, Kick Handling, Managed Pressure Drilling, Underbalanced Drilling, Automatic Control, Estimation, PDE-ODE model, Severe Slugging, Flow Assurance, Riser Gas

---

1. Introduction

Multi-phase flow simulation models have evolved significantly over the last couple of decades. With the increase in computational power and sophistication of numerical schemes, simulating two-phase pipe flow no longer suffers the same limitations on computational size, and state of the art high-fidelity models such as OLGA [10] and LedaFlow [18] typically run many times faster than real-time on a standard desktop computer.

Before this development, however, significant efforts were devoted to obtaining simplifications of multi-phase flow models which could ease implementation and increase their simulation speed. The Drift Flux Model (DFM) [33] was first proposed by Zuber and Findlay [51] as a correlation for predicting steady-state void-fraction profiles and later used in transient representations of two-phase flow [42]. In this form it is a simplification of the transient two-fluid model obtained by relaxing (i.e. imposing immediate steady-state on [29]) the dynamic momentum equation of each phase, replacing them with a mixture momentum equation and a static relation typically called a *slip law*.

Further simplification can be achieved by using a similar approach to other parts of the dynamics deemed insignificant for the application at hand. Specifically, by imposing steady state on the momentum balance, the pressure wave dynamics are neglected, yielding so-called "No Pressure Wave" (NPW) models or "Reduced DFMs". This simplification is motivated by applications for which slow gas propagation dynamics are more critical than fast pressure wave propagation. Furthermore, it has been shown that the validity of the Drift-Flux models representation of the fast pressure dynamics is imprecise in many scenarios due to the relaxations involved in obtaining the DFM from the full

*Corresponding Author
Email address: `ulf.jakob.aarsnes@itk.ntnu.no` (Ulf Jakob F. Aarsnes)
[1]Now with IRIS, Stavanger, Norway.

formulation of Baer and Nunziato [8], which lowers the sonic velocity [29, 36]. Thus, if the "medium" complexity DFM representation of the pressure waves is imprecise, the argument can be made that they could be discarded.

This approach was used by Taitel et al. [49] where the resulting model was described by a single transient PDE of the liquid continuity, obtained by assuming incompressible liquid, and a set of steady-state relations. The resulting model was further investigated by Minami and Shoham [40] where it was found to be amenable for certain scenarios. The approach was expanded upon by Taitel and Barnea [48], where the assumption of incompressible liquid was dropped, yielding two transient equations. A similar model was investigated by Masella et al. [39], here called the "No Pressure Wave" (NPW) model. More recent additions to the literature on models using quasi-equilibrium momentum balance include Choi et al. [16], Aarsnes et al. [2], Ambrus et al. [5].

Interestingly, many of these recent studies have not been motivated by the desire to reduce computational complexity. Rather, the advent of computerized automation and optimization in the oil and gas industry has created new applications for various forms of simplified models, causing renewed interest in these models.

1.1. Application

Modern advances in the theory of dynamic systems have the potential of improving robustness and performance in the monitoring, optimization and control of dynamic processes which can be described by an amenable mathematical model. By intelligently combining predictions from the mathematical model with information from multiple sensors one can estimate unmeasured quantities, optimize automatic control procedures, predict future behavior, and plan countermeasures for unwanted incidents. Such design techniques, often referred to as model-based estimation and control [7, 6], require a mathematical model with the proper balance between complexity and fidelity, i.e. the complexity must be limited to facilitate the use of established mathematical analysis and design techniques, while the qualitative response of the process is retained.

Models that achieve such balance between complexity and fidelity are sometimes referred to as fit-for-purpose models. Obtaining such models often proves difficult for gas-liquid two-phase dynamics due to the significant complexity and distributed nature of multi-phase pipe flow [3, 4].

If the appropriate model can be developed, however, it could see a wide range of uses in model-based control and estimation applications where two-phase pipe flow is encountered, such as underbalanced drilling of oil and gas wells [44], well control (both in conventional and Managed Pressure Drilling) [15], riser gas handling [32], hydrocarbon production monitoring [13, 50] and mitigating severe slugging during hydrocarbon production [22, 23, 20].

2. The Drift Flux Model

A popular model for representing one-dimensional two-phase flow dynamics in drilling and production at an acceptable fidelity is the classical three-state transient Drift Flux Model (DFM), see e.g. Lage and Time [35], Fjelde et al. [28], Aarsnes et al. [3].

For certain boundary conditions, the existence of solutions has been proven [26, 27], and it is well known that the DFM is, in most practical situations, hyperbolic, with three (two fast and one slow) characteristic velocities [19]. The two fast characteristics represent the fast pressure dynamics in the pipe, while the slow characteristic velocity is associated with the transport of matter, also sometimes referred to as the void wave [37, 39].

In this section we restate the classical equations of the transient drift-flux model and then cast the system in canonical form using the eigenvectors of the transport matrix, which poses the model as a single Riemann invariant governing the propagation of the void wave, coupled to the pressure dynamics, given by two PDEs, through the gas velocity. We then show how the approximation employed by e.g. Masella et al. [39], Choi et al. [16], using a static relation in place of a dynamic momentum balance, is related to relaxing both of the two PDEs describing the pressure dynamics. Both approaches lead to a mixed hyperbolic/parabolic system with a single hyperbolic PDE with a finite eigenvalue.

2.1. The Drift Flux Model equations

We start the development of the proposed two-phase model from the classical Drift Flux Model (DFM) formulation, described by the following equations [30, 27]:

$$\frac{\partial(\alpha_L\rho_L)}{\partial t} + \frac{\partial(\alpha_L\rho_L v_L)}{\partial x} = \Gamma_L, \tag{1}$$

$$\frac{\partial(\alpha_G\rho_G)}{\partial t} + \frac{\partial(\alpha_G\rho_G v_G)}{\partial x} = \Gamma_G, \tag{2}$$

$$\frac{\partial(\alpha_L\rho_L v_L + \alpha_G\rho_G v_G)}{\partial t} + \frac{\partial(P + \alpha_G\rho_G v_G^2 + \alpha_L\rho_L v_L^2)}{\partial x} = S, \tag{3}$$

where the independent variables t, x represent time and position along the pipe, respectively, and the momentum source term, S is typically given as

$$S = -\rho_m g \sin\theta(x) - \frac{2f\rho_m v_m|v_m|}{D} \tag{4}$$

with the mixture relations

$$\rho_m = \alpha_G\rho_G + \alpha_L\rho_L, \qquad v_m = \alpha_G v_G + \alpha_L v_L, \tag{5}$$

and where $\alpha_i, v_i, \rho_i, \Gamma_i$ denote the volume fraction, velocity, density and mass source term, respectively, of phase $i = G, L$ (gas or liquid). Finally, f is the friction coefficient, D the hydraulic diameter, g is the acceleration of gravity and θ is the pipe inclination angle (relative to the horizontal). For the remainder of this section we will assume $\Gamma_L = \Gamma_G = 0$.

Eqs. (1)-(2) represent the mass balance for the liquid and gas phases, while (3) is the conservation of momentum for the gas-liquid mixture.

The following closure relations are needed to complete the system:

$$\alpha_L + \alpha_G = 1, \qquad P = c_G^2(T)\rho_G, \tag{6}$$

where P is the pressure, and $c_G(T)$ is the speed of sound in the gas as a function of the temperature T, while the liquid density is assumed constant. Finally the slip law

$$v_G = \frac{v_m}{1-\alpha_L^*} + v_\infty = C_0 v_m + v_\infty \tag{7}$$

where the profile parameter $\alpha_L{}^* \in [0, 1)$, usually given as the distribution parameter $C_0 = 1/(1-\alpha_L^*)$, and drift parameter $v_\infty \geq 0$ determine the relative velocity between the phases. These parameters typically depend on factors such as superficial velocities and inclination [46]. Multiple correlations for obtaining α_L^*, v_∞ exist in the literature, see e.g. [51, 12, 17].

2.2. Canonical form

The goal of the following derivation is to show that when the distributed pressure dynamics are relaxed, the remaining dynamic equation is a single PDE describing the propagation of a void wave with a velocity given by a static relation. This is an interesting result because it helps focus the search for a simplified model by noting that, by discarding the distributed pressure dynamics, the model essentially only requires two parts:

1. A first-order PDE describing the void wave advection.
2. A set of closure relations giving pressure and velocity as a function of the state used in 1.

This result will motivate the approach taken in Section 3.

2.2.1. Variable change

To better highlight interesting features of the model, we rewrite (1)–(3) using a transformation in accordance with [30] to obtain a new set of variables

$$(\chi_L, \rho, v_G) = \left(\frac{(\alpha_L - \alpha_L^*)\rho_L}{\rho_m - \alpha_L^*\rho_L}, \rho_m - \alpha_L^*\rho_L, v_G \right). \tag{8}$$

The resulting equations allow the quasilinear formulation[2]

$$\frac{\partial \mathbf{u}}{\partial t} + A(\mathbf{u})\frac{\partial \mathbf{u}}{\partial x} = \mathbf{Q}(\mathbf{u}), \qquad \mathbf{u} = \begin{bmatrix} \chi_L \\ \rho \\ v_G \end{bmatrix}, \tag{9}$$

with $A(\mathbf{u})$ given as

$$A(\mathbf{u}) = \begin{bmatrix} v_G & 0 & 0 \\ 0 & v_G & \rho \\ A_{31}(\mathbf{u}) & A_{32}(\mathbf{u}) & A_{33}(\mathbf{u}) \end{bmatrix}, \tag{10}$$

$$A_{31}(\mathbf{u}) \equiv c_G^2 \frac{\rho_G(\mathbf{u}) - \rho_L}{\alpha_G(\mathbf{u})\rho_L} - (v_G - v_L(\mathbf{u}))^2, \tag{11}$$

$$A_{32}(\mathbf{u}) \equiv c_G^2 \frac{(1 - \alpha_L^*)\rho_G(\mathbf{u})}{\alpha_G(\mathbf{u})\rho^2} - (v_G - v_L(\mathbf{u}))^2 \frac{\chi_L}{\rho}, \tag{12}$$

$$A_{33}(\mathbf{u}) \equiv v_G - 2\chi_L(v_G - v_L(\mathbf{u})), \tag{13}$$

and

$$\mathbf{Q}(\mathbf{u}) = \begin{bmatrix} 0 \\ 0 \\ Q(\mathbf{u}) \end{bmatrix}, \tag{14}$$

$$Q(\mathbf{u}) = -\left(1 + \frac{\alpha_L^*\rho_L}{\rho}\right)\left(g \sin\theta + \frac{2f((1-\alpha_L^*)v_G - v_\infty)|(1-\alpha_L^*)v_G - v_\infty|}{D}\right), \tag{15}$$

where all dependent variables are in boldface.

The first state χ_L is a *Riemann invariant*: it satisfies a pure transport equation with the velocity v_G. The eigenvalues of the transport matrix, $A(\mathbf{u})$, are [19]:

$$\begin{bmatrix} \lambda_1 \\ \lambda_2 \\ \lambda_3 \end{bmatrix} = \begin{bmatrix} v_G \\ v_G + \chi_L(v_L(\mathbf{u}) - v_G) + c_M(\mathbf{u}) \\ v_G + \chi_L(v_L(\mathbf{u}) - v_G) - c_M(\mathbf{u}) \end{bmatrix}, \tag{16}$$

with the mixture sound velocity

$$c_M(\mathbf{u}) = \sqrt{\chi_L(\chi_L - 1)(v_G - v_L(\mathbf{u}))^2 + \frac{(1-\alpha_L^*)c_G^2\rho_G(\mathbf{u})}{\alpha_G(\mathbf{u})\rho}}, \tag{17}$$

and the left eigenvectors

$$\begin{bmatrix} l_1 \\ l_2 \\ l_3 \end{bmatrix} = \begin{bmatrix} 1 & 0 & 0 \\ \frac{A_{31}(\mathbf{u})}{A_{32}(\mathbf{u})} & 1 & \frac{\rho}{\chi_L(v_G - v_L(\mathbf{u})) + c_M(\mathbf{u})} \\ \frac{A_{31}(\mathbf{u})}{A_{32}(\mathbf{u})} & 1 & \frac{\rho}{\chi_L(v_G - v_L(\mathbf{u})) - c_M(\mathbf{u})} \end{bmatrix}. \tag{18}$$

[2]This relation, and other derivations in this section, are best found using symbolic computation software.

We note from this derivation that v_G shows up as an eigenvalue in the transport matrix and that the void wave dynamics are relatively simple due to our state transformation. The relations for the fast pressure dynamics are much more complicated and challenging to work with. In particular, finding a diagonalizing transformation of the system is not feasible, if at all possible.

2.3. Relaxation of the distributed pressure dynamics

Multiplying (9) with the left eigenvectors yields:

$$l_1(\mathbf{u})\Big[\frac{\partial \mathbf{u}}{\partial t} + \lambda_1(\mathbf{u})\frac{\partial \mathbf{u}}{\partial x} - \mathbf{Q}(\mathbf{u})\Big] = 0 \tag{19}$$

$$l_2(\mathbf{u})\Big[\frac{\partial \mathbf{u}}{\partial t} + \lambda_2(\mathbf{u})\frac{\partial \mathbf{u}}{\partial x} - \mathbf{Q}(\mathbf{u})\Big] = 0 \tag{20}$$

$$l_3(\mathbf{u})\Big[\frac{\partial \mathbf{u}}{\partial t} + \lambda_3(\mathbf{u})\frac{\partial \mathbf{u}}{\partial x} - \mathbf{Q}(\mathbf{u})\Big] = 0. \tag{21}$$

Following [19], we proceed to a model reduction analogous to singular perturbation techniques. Indeed, eigenvalues λ_2 and λ_3 correspond to sound wave propagation (see, e.g. [39, 37]) and are at least one order of magnitude greater than λ_1, which corresponds to the transport of the pseudo-holdup χ_L. This suggests that the fast transport dynamics corresponding to (20) and (21) can be relaxed when concerned with the slower time-scale of the void–wave Eq. (19). Imposing instantaneous steady state for (20) and (21) yields:

$$l_1(\mathbf{u})\Big[\frac{\partial \mathbf{u}}{\partial t} + \lambda_1(\mathbf{u})\frac{\partial \mathbf{u}}{\partial x} - \mathbf{Q}(\mathbf{u})\Big] = 0 \tag{22}$$

$$l_2(\mathbf{u})\Big[\lambda_2(\mathbf{u})\frac{\partial \mathbf{u}}{\partial x} - \mathbf{Q}(\mathbf{u})\Big] = 0 \tag{23}$$

$$l_3(\mathbf{u})\Big[\lambda_3(\mathbf{u})\frac{\partial \mathbf{u}}{\partial x} - \mathbf{Q}(\mathbf{u})\Big] = 0, \tag{24}$$

where by inserting for the eigenvectors and eigenvalues we can write the resulting system as

$$\frac{\partial \chi_L}{\partial t} + v_G\frac{\partial \chi_L}{\partial x} = 0 \tag{25}$$

$$\frac{\partial \rho}{\partial x} = -\frac{A_{31}(\mathbf{u})}{A_{32}(\mathbf{u})}\frac{\partial \chi_L}{\partial x} + \frac{\rho Q(\mathbf{u})}{A_{32}(\mathbf{u})\rho - A_{33}(\mathbf{u})v_G}. \tag{26}$$

$$\frac{\partial v_G}{\partial x} = \frac{v_G Q(\mathbf{u})}{A_{33}(\mathbf{u})v_G - A_{32}(\mathbf{u})\rho} \tag{27}$$

χ_L is still a Riemann invariant in the reduced system propagating with velocity v_G given implicitly by the relations (26)–(27). We note that the remaining dynamics of the model are contained in Eq. (25), while (26)–(27) are static relations which can possibly be approximated with simpler closure relations.

2.3.1. Relation to the No-Pressure-Wave Model

In [39] and [16] a reduced DFM referred to as the *No Pressure Wave* (NPW) model is obtained by removing the time derivative term in (3) and computing the pressure from the resulting static relation. Consider again the original set of equations (1)–(2) but in place of the mixture momentum equation (3) use the static force balance

$$\frac{\partial P}{\partial x} = S. \tag{28}$$

In [39] it is noted that the resulting model has a single finite eigenvalue, and that the remaining two states corresponds to eigenvalues that are infinite, which is similar to the system of (25)–(27). This means that using (28) in place of (3) effectively relaxes both the two characteristics associated with the fast pressure waves. Hence, using a simpler approximation in place of the expressions for ρ, v_G it is possible to obtain a simple first-order PDE of the two-phase flow dynamics. In the following we exploit these facts to develop such a simple representation of the void wave propagation that remains when the pressure dynamics have been relaxed.

2.3.2. New Approach

An approach to exploit the structure revealed by (25)–(27) was suggested in [2] where a simplified model representation of these relaxed dynamics was developed. The problem with this approach is that pressure is given implicitly in the states (due to the source term) such that the resulting simulation requires the solution of an ODE for every time-step. This problem is avoided in the present paper by using α_G as the distributed state in place of χ_L, which allows for finding an *approximate* relation for the pressure gradient which yields pressure explicit in the states and exogenous variables.

More specifically the pseudo-holdup,

$$\chi_L = \frac{(\alpha_L - \alpha_L^*)\rho_L}{\rho_m - \alpha_L^*\rho_L}, \tag{29}$$

changes according to:

$$\mathrm{d}\chi_L = \frac{\rho_G(\alpha_L^* - 1)\mathrm{d}\alpha_G + \alpha_G(\alpha_G + \alpha_L^* - 1)\mathrm{d}\rho_G}{(\alpha_G\rho_G - \rho_L(\alpha_G + \alpha_L^* - 1))^2}. \tag{30}$$

Plugging (30) into (25) we get the equation:

$$\frac{\partial \alpha_G}{\partial t} + v_G\frac{\partial \alpha_G}{\partial x} = -\frac{\alpha_G(\alpha_G + \alpha_L^* - 1)}{\rho_G(\alpha_L^* - 1)}\left(\frac{\partial \rho_G}{\partial t} + v_G\frac{\partial \rho_G}{\partial x}\right) \tag{31}$$

where ρ_G is given by the pressure. This motivates the approach taken in the following section.

3. Derivation of the new formulation

The full three-state drift-flux model is too complicated for most model-based estimation and control approaches [1], hence simplification is desirable. Based on the analysis of the previous section we argue that when relaxing the fast pressure dynamics, it should be possible to reduce the model description to a first-order PDE, while still retaining the qualitative dynamics of the system.

For this derivation we will again start with the classical Drift Flux formulation (1)–(7). First note the relation from the slip law (7):

$$\alpha_L v_L = (\alpha_L - \alpha_L^*)v_G - (1 - \alpha_L^*)v_\infty. \tag{32}$$

Following Gavrilyuk and Fabre [30], divide (1) by ρ_L, which we recall was assumed constant, and insert (32) to get

$$\frac{\partial \alpha_L}{\partial t} + \frac{\partial(\alpha_L - \alpha_L^*)v_G}{\partial x} = \frac{\Gamma_L}{\rho_L} \tag{33}$$

$$\implies \frac{\partial \alpha_G}{\partial t} + v_G\frac{\partial \alpha_G}{\partial x} = (\alpha_L - \alpha_L^*)\frac{\partial v_G}{\partial x} - \frac{\Gamma_L}{\rho_L} \tag{34}$$

where the first term on the RHS of (34) is due to gas expansion which necessarily translates to acceleration of the gas.

Employing the chain rule on (2) we have

$$\frac{\partial v_G}{\partial x} = \frac{\Gamma_G}{\alpha_G\rho_G} - \frac{1}{\alpha_G\rho_G}\left(\frac{\partial \alpha_G\rho_G}{\partial t} + v_G\frac{\partial \alpha_G\rho_G}{\partial x}\right) \tag{35}$$

$$= \frac{\Gamma_G}{\alpha_G\rho_G} - \frac{1}{\rho_G}\left(\frac{\partial \rho_G}{\partial t} + v_G\frac{\partial \rho_G}{\partial x}\right) - \frac{1}{\alpha_G}\left(\frac{\partial \alpha_G}{\partial t} + v_G\frac{\partial \alpha_G}{\partial x}\right). \tag{36}$$

Inserting (36) into (34)

$$\frac{\partial \alpha_G}{\partial t}\left(1+\frac{\alpha_L-\alpha_L^*}{\alpha_G}\right)+v_G\frac{\partial \alpha_G}{\partial x}\left(1+\frac{\alpha_L-\alpha_L^*}{\alpha_G}\right)$$
$$=(\alpha_L-\alpha_L^*)\frac{\Gamma_G}{\alpha_G\rho_G}-\frac{(\alpha_L-\alpha_L^*)}{\rho_G}\left(\frac{\partial \rho_G}{\partial t}+v_G\frac{\partial \rho_G}{\partial x}\right). \tag{37}$$

Thus, defining the convenience variable E_G:

$$E_G \equiv -\frac{\alpha_G(\alpha_L-\alpha_L^*)}{(1-\alpha_L^*)\rho_G}\left(\frac{\partial \rho_G}{\partial t}+v_G\frac{\partial \rho_G}{\partial x}\right), \tag{38}$$

we have from (37)

$$\frac{\partial \alpha_G}{\partial t}+v_G\frac{\partial \alpha_G}{\partial x}=E_G+\frac{1}{1-\alpha_L^*}\left((\alpha_L-\alpha_L^*)\frac{\Gamma_G}{\rho_G}-\alpha_G\frac{\Gamma_L}{\rho_L}\right). \tag{39}$$

Then, defining the source terms Γ_G^*, Γ_L^*:

$$\Gamma_G^* \equiv \frac{\alpha_L-\alpha_L^*}{(1-\alpha_L^*)\rho_G}\Gamma_G, \quad \Gamma_L^* \equiv \frac{\alpha_G}{(1-\alpha_L^*)\rho_L}\Gamma_L, \tag{40}$$

we have

$$\frac{\partial \alpha_G}{\partial t}+v_G\frac{\partial \alpha_G}{\partial x}=E_G+\Gamma_G^*-\Gamma_L^*. \tag{41}$$

In (41) the source terms Γ_G^*, Γ_L^* can represent liquid or gas injection sources, and also mass transfer terms. However, to properly account for gas dissolution into the liquid phase, an additional mass balance for the dissolved gas would have to be added. Without this, the model is limited to cases where gas solubility is low or negligible.

3.1. Pressure profile

The distributed, quasi-steady pressure is obtained from (28) and the pressure boundary condition $P(x{=}L) = P_L$:

$$P(x)=P_L+\int_L^x S(\xi)\mathrm{d}\xi. \tag{42}$$

This expression is implicit in that it is dependent on v_m which is in turn dependent on $E_G(P)$, and $\rho_G(P)$. To avoid this complication a simplification should be used, e.g. by assuming v_m uniform in space when calculating the pressure profile. Essentially, what is modeled is

$$P(x)=P_L+F(x)+G(x), \tag{43}$$

where $F(x), G(x)$ is the frictional pressure drop and hydrostatic pressure.

Let q_L, q_G denote the exogenous variables liquid, respectively gas, volumetric flow rates entering at the left boundary. Then, one possible approximation of (4) is

$$S(x)\approx -\bar{\rho}_m(x)\left(g\sin\theta(x)+\frac{2f(q_G+q_L)|q_G+q_L|}{A^2D}\right), \tag{44}$$
$$\bar{\rho}_m=(\rho_L\alpha_L(x)+\bar{\rho}_G\alpha_G(x)), \tag{45}$$

i.e. a mean approximate gas density is used. This makes the source term S explicit in the state α_G and the exogenous variables. The approximation gives good results for cases where the gas mass is small relative to the liquid mass, $\alpha_G\rho_G \ll \alpha_L\rho_L$. If this assumption is not satisfied, any other approximation, explicit in the state and exogenous variables, can be used.

The approximation $v_m \approx \frac{q_G+q_L}{A}$ will clearly cause an under-prediction of frictional pressure drop when there is significant amount of gas expansion causing acceleration of the gas phase. This can to some degree be amended by tuning the friction coefficient f in (44).

It should be noted that by discarding the transient pressure characteristics, it can be difficult to enforce certain kinds of top side (right) boundary conditions. This is due to the fact that we no longer have characteristics traveling from the right to the left and consequently, strictly speaking, no right boundary condition. In particular a vertical pipe without flow at the boundaries, tending to phase separation, would be difficult to replicate (e.g. a shut-in oil and gas well).

3.2. Boundary condition and velocity profile

Defining at the inlet (at the left boundary) $v_{G0} \equiv v_G(x{=}0, t)$, we have from (7):

$$v_{G0} = \frac{C_0}{A}(q_G + q_L) + v_\infty. \tag{46}$$

The left boundary condition of (41) is given as

$$\alpha_G(x{=}0, t) = \frac{q_G}{A v_{G0}}, \tag{47}$$

The velocity gradient is obtained by combining (36) and (41):

$$\frac{\partial v_G}{\partial x} = \frac{E_G + \Gamma_G^* - \Gamma_L^* + \Gamma_L/\rho_L}{\alpha_L - \alpha_L^*}, \tag{48}$$

$$= \frac{E_G + \Gamma_G^*}{\alpha_L - \alpha_L^*} + \frac{1}{1 - \alpha_L^*}\frac{\Gamma_L}{\rho_L}. \tag{49}$$

Now note the relation for the gas density in (6). In the following we will limit the model to a more specific relation of the form

$$\frac{\rho_G^\gamma}{P} = C, \tag{50}$$

which is obtained by assuming adiabatic gas expansion with γ the adiabatic gas constant, and C a constant. In differential form, we can write (50) as

$$\gamma \rho_G^{\gamma-1} \mathrm{d}\rho_G = C \mathrm{d}P, \tag{51}$$

and substituting the value of C from (50), we further have:

$$\frac{\mathrm{d}\rho_G}{\rho_G} = \frac{\mathrm{d}P}{\gamma P}. \tag{52}$$

Note that the term γP is equivalent to the isentropic bulk modulus of an ideal gas. Eq. (52) allows us to recast (38) in terms of the pressure profile, $P(x)$:

$$E_G = -\frac{\alpha_G(1 - C_0\alpha_G)}{\gamma P}\left(\frac{\partial P}{\partial t} + v_G \frac{\partial P}{\partial x}\right), \tag{53}$$

For deriving the velocity, we neglect the $\frac{\partial P}{\partial t}$ term from (53). This assumption may cause transient errors in the computed gas velocity, especially when large pressure changes occur at the boundary, e.g. due to the opening or closing of a choke valve. Then, inserting (40) and (53), without the transient pressure term, into (49)

$$\frac{\partial v_G}{\partial x} = C_0\left(-\frac{\alpha_G v_G}{P\gamma}S + \frac{c_G^2}{P\gamma}\Gamma_G + \frac{1}{\rho_L}\Gamma_L\right), \tag{54}$$

and consequently, by defining the integral

$$I_v(x) = \int_0^x \frac{C_0\alpha_G(\xi)}{P(\xi)\gamma} S(\xi)\mathrm{d}\xi, \tag{55}$$

the distributed velocity is obtained as

$$\begin{aligned} v_G(x) =& e^{-I_v(x)}\Bigg(v_{G0}+ \\ & C_0\int\limits_0^x \left(\frac{c_G^2(\zeta)}{P(\zeta)\gamma}\Gamma_G(\zeta) + \frac{1}{\rho_L}\Gamma_L(\zeta)\right)e^{I_{v_G}(\zeta)}\mathrm{d}\zeta\Bigg). \end{aligned} \tag{56}$$

3.3. Lumped pressure dynamics

For the case when the pressure at the topside boundary is exogenous, the equations in the previous sections give a complete description of the simplified two-phase flow model. In many cases, however, the topside boundary pressure (i.e. at $x = L$) is indirectly determined by additional dynamics, e.g. when controlling pressure with a choke valve in a broad range of oil and gas related applications, e.g. Managed Pressure Drilling [31, 34], underbalanced drilling [44], and hydrocarbon production [21], to name a few examples.

To model this scenario we use a lumped expression for the pressure dynamics. Considering the pipe as a single control volume, and applying the mass conservation law:

$$\frac{\partial P_L}{\partial t} = \frac{\beta_L}{V}\left(q_L + q_G + T_{E_G} - q_c\right), \tag{57}$$

with q_c the volumetric flow rate through the choke, and T_{E_G} the effect of in-domain gas expansion on the lumped pressure dynamics. The term T_{E_G} can be found by integrating the gradient of the gas velocity along the well. Including the $\frac{\partial\rho_G}{\partial t}$ term in (38), T_{E_G} can be written as:

$$T_{E_G} = A\int_0^L \frac{E_G + \Gamma_G^*}{\alpha_L - \alpha_L^*} + \frac{1}{1-\alpha_L^*}\frac{\Gamma_L}{\rho_L}\mathrm{d}x. \tag{58}$$

We will now show that the total gas expansion, T_{E_G}, can be split into a term affecting the effective bulk modulus of the gas-liquid mixture, $\bar{\beta}$, and a remaining term, T_{XE}, accounting for source terms and the gas expansion when propagating through the negative pressure gradient.

Express the gas expansion dynamics in the principal variables:

$$E_G = -\frac{\alpha_G(\alpha_L - \alpha_L^*)}{(1-\alpha_L^*)\gamma P}\left(\frac{\partial P}{\partial t} + v_G\frac{\partial P}{\partial x}\right), \tag{59}$$

$$\frac{\partial P(x,t)}{\partial x} = S(x), \tag{60}$$

$$\frac{\partial P(x,t)}{\partial t} \approx \frac{\partial P_L}{\partial t} = \frac{\beta_L}{V}\left(q_L + q_G + T_{E_G} - q_c\right), \tag{61}$$

and consequently the T_{EG} term can be split into a term which includes $\frac{\partial P_L}{\partial t}$ and a remainder

$$T_{E_G} = T_{XE} - A\int_0^L \frac{C_0\alpha_G}{\gamma P}\mathrm{d}x\frac{\partial P_L}{\partial t}, \tag{62}$$

$$T_{XE} = A(v_G(L) - v_{G0}), \tag{63}$$

where we have used the fact that the remainder equals the integrated velocity gradient with the $\frac{\partial\rho_G}{\partial t}$ term excluded.

Inserting the total gas expansion (62) into the pressure dynamics (57):

$$\frac{\partial P_L}{\partial t} = \frac{\beta_L}{V}\left(q_L + q_G - q_c - T_{XE} - A\int_0^L \frac{C_0\alpha_G}{\gamma P}\mathrm{d}x\frac{\partial P_L}{\partial t}\right), \tag{64}$$

Table 1: The complete Simplified Two-Phase Model

Pressure dynamics:

$$\frac{\partial}{\partial t}P_L(t) = \frac{\bar{\beta}(t)}{V}(q_L(t) + q_G(t) - q_c(t) + T_{XE}(t)), \quad (68)$$

$$T_{XE}(t) = A(v_G(L,t) - v_{G0}(t)), \quad (69)$$

$$\bar{\beta}(t) \equiv \frac{\beta_L}{1 + \frac{\beta_L}{L}\int_0^L \frac{C_0\alpha_G(x,t)}{\gamma P(x,t)}\mathrm{d}x}, \quad (70)$$

Distributed dynamics:

$$\frac{\partial}{\partial t}\alpha_G(x,t) + v_G(x,t)\frac{\partial}{\partial x}\alpha_G(x,t) = E_G(x,t) + \Gamma_G^*(x,t) - \Gamma_L^*(x,t), \quad (71)$$

$$\alpha_G(x{=}0,t) = \frac{q_G(t)}{C_0(q_G(t) + q_L(t)) + Av_\infty}. \quad (72)$$

$$\Gamma_G^*(x,t) \equiv \frac{1 - C_0\alpha_G(x,t)}{\rho_G(x,t)}\Gamma_G(x,t), \quad (73)$$

$$\Gamma_L^*(x,t) \equiv \frac{C_0\alpha_G(x,t)}{\rho_L}\Gamma_L(x,t), \quad (74)$$

Closure relations:

$$\bar{S}(x,t) = -\bar{\rho}_m(x,t)\left(g\sin\theta(x) + \frac{2f(q_G(t) + q_L(t)|q_G(t) + q_L(t)|}{A^2D}\right), \quad (75)$$

$$\bar{\rho}_m = \rho_L\alpha_L(x,t) + \bar{\rho}_G\alpha_G(x,t), \quad (76)$$

$$P(x,t) = P_L(t) + \int_L^x \bar{S}(\xi,t)\mathrm{d}\xi, \quad (77)$$

$$v_G(x,t) = e^{-I_v(x,t)}\left(v_{G0}(t) + C_0\int_0^x\left(\frac{c_G^2}{P(\zeta,t)\gamma}\Gamma_G(\zeta,t) + \frac{1}{\rho_L}\Gamma_L(\zeta,t)\right)e^{I_{v_G}(\zeta,t)}\mathrm{d}\zeta\right), \quad (78)$$

$$I_v(x,t) = \int_0^x \frac{C_0\alpha_G(\xi,t)}{P(\xi,t)\gamma}\bar{S}(\xi,t)\mathrm{d}\xi, \quad (79)$$

$$v_{G0}(t) \equiv \frac{C_0}{A}(q_G(t) + q_L(t)) + v_\infty. \quad (80)$$

$$E_G(x,t) \equiv -\frac{\alpha_G(x,t)(1 - C_0\alpha_G(x,t))}{\gamma P(x,t)}\left(\frac{\partial}{\partial t}P_L(t) + v_G(x,t)\bar{S}(x,t)\right), \quad (81)$$

we get

$$\frac{\partial P_L}{\partial t}\left(1 + \frac{\beta_L}{L}\int_0^L \frac{C_0\alpha_G}{\gamma P}\mathrm{d}x\right) = \frac{\beta_L}{V}(q_L + q_G - q_c + T_{XE}), \quad (65)$$

hence

$$\frac{\partial P_L}{\partial t} = \frac{\bar{\beta}}{V}(q_L + q_G - q_c + T_{XE}), \quad (66)$$

$$\bar{\beta} \equiv \frac{\beta_L}{1 + \frac{\beta_L}{L}\int_0^L \frac{C_0\alpha_G}{\gamma P}\mathrm{d}x}, \quad (67)$$

where we have defined the effective bulk modulus $\bar{\beta}$.

The complete model is restated in Table 1 for convenience.

4. Some Numerical Examples

In this section two numerical examples are considered. The first one highlights the effect of removing the pressure dynamics, while the second numerical example illustrates the feasibility of employing the model to a typical scenario from underbalanced drilling (described in the following).

For both scenarios we consider a 1000-meter long domain with $c_G = 300\ m/s$, $\rho_L = 1000\ kg/m^3$, $v_\infty = \alpha_L^* = 0$. The full Drift-Flux model equations (1)–(3) are implemented with the AUSM scheme of [24] and time step $\Delta t = \Delta x/1500$, while the PDE of the simplified model is implemented with a first-order upwind scheme with time step $\Delta t = \Delta x/100$ and the integrals evaluated with trapezoidal quadrature. Different time steps are used due to the different requirements of the CFL condition with and without the inclusion of the distributed pressure dynamics. In both cases a grid size of Δx=1 meters are used.

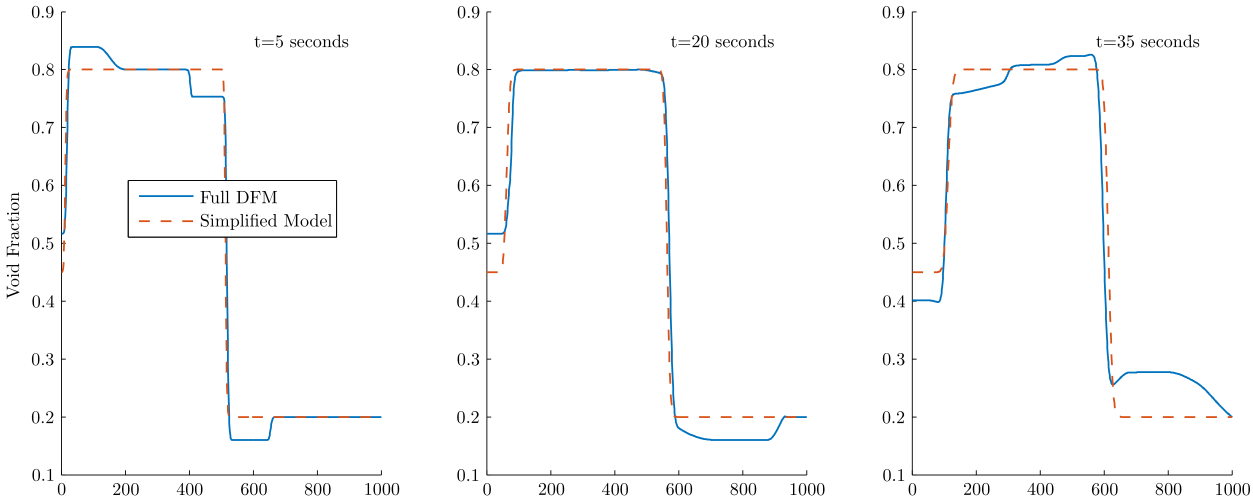

Figure 1: Shock tube test with all source terms set to zero. The pressure dynamics, discarded in the relaxed model, causes the full model to oscillate around the trajectory of the relaxed model. With no source terms to drive the pressure dynamics to the equilibrium, these oscillations would in theory continue indefinitely, although here the effect of numerical diffusion can be seen.

4.1. Example 1: shock tube

We initially investigate the model in a so-called shock tube scenario, see [24]. The source terms are set to zero, corresponding to a frictionless horizontal tube, and the simulation is initialized with the domain split in half with $\alpha_G = 0.2$ and $\alpha_G = 0.8$ for the right and left domain respectively, and with a right boundary condition of $P(x{=}L) = 1$ bar.

The simulation results are shown in Fig. 1, where the void wave can be seen propagating towards the right while the faster pressure waves in the full DFM travel back and forth in the domain, being reflected at the boundaries. These pressure oscillations cause perturbations in the void fraction around the *nominal* trajectory followed by the simplified model.

4.2. Example 2: underbalanced drilling connection

Next we consider a scenario relevant for the potential application of the model to underbalanced drilling. In underbalanced drilling the pressure in the lowermost section of the well (which is exposed to the reservoir) is deliberately kept below the reservoir pressure thus allowing influx of fluid while drilling. While underbalanced drilling has several benefits [11], it also entails challenges in the form of more complicated dynamic behavior due to the two-phase flow and well-reservoir interaction [4].

When performing a pipe connection in a vertical well, the liquid injection through the drillstring (at the left boundary) is stopped and the topside back-pressure choke valve opening is reduced so as to try to maintain a constant bottom-hole pressure [44, 41]. Monitoring and controlling this operation effectively is of importance both for maintaining reservoir and well integrity, as well as for enabling characterization of the reservoir productivity and pore pressure while drilling [47, 45].

For this scenario, we include the lumped pressure dynamics of Section 3.3 where the flow out rate, q_c, is found from the multi-phase choke relation from [3]. On the left boundary, a constant gas injection rate is applied while the liquid rate and choke opening are varied according to Fig. 2.

The pressure trends in Fig. 2 and void profiles in Fig. 3 show the model's ability to qualitatively represent the essential dynamics for control and estimation applications in this scenario. We do, however, note the following errors and their causes:

- The steady state error in the downhole pressure $P(x{=}0)$ is due to the approximated momentum source term (44), in particular the failure of the approximation to account for the increased frictional pressure loss due to increase in gas velocity towards the rightmost part of the domain. This error can easily be amended by tuning the friction coefficient f.

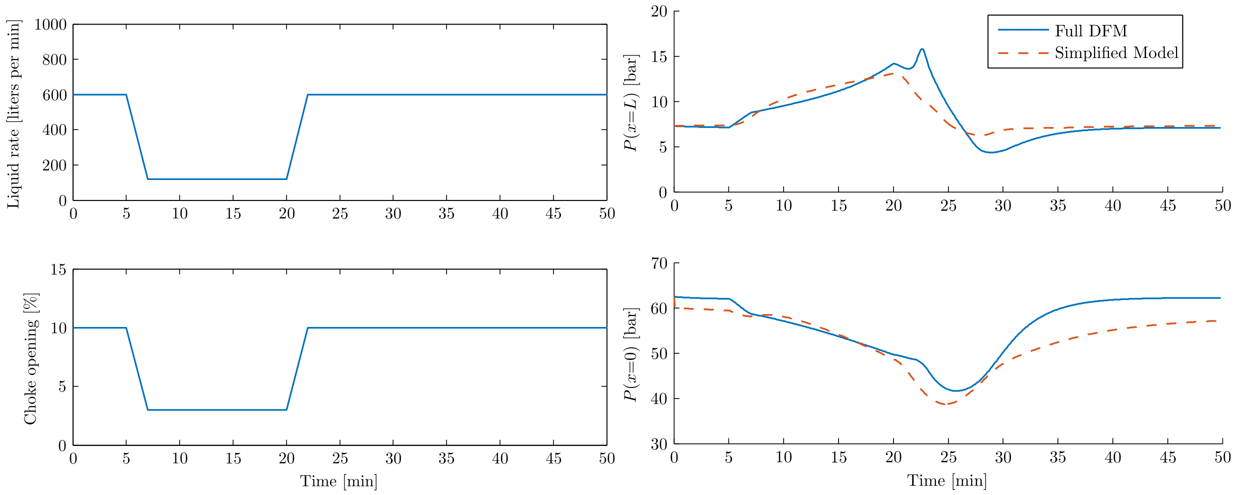

Figure 2: Trends of the changing exogenous variables (**left**) and the topside and bottom-hole pressures (**right**) during the connection scenario.

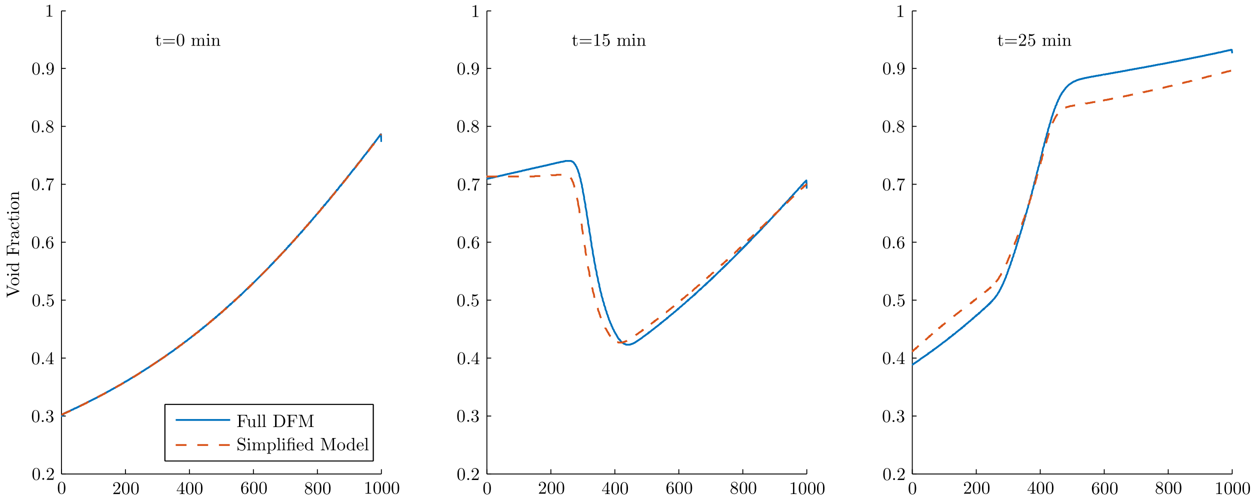

Figure 3: Void fraction profiles before, during and after the connection.

- A significant transient error can be seen during the time periods 5–15 minutes, and 20–30 minutes. This error seems to be connected to the change in pressure at the right boundary which is not taken into account when the velocity profile is computed, see (54). This means that the simplified model over- and under-predicts the gas velocity, respectively in each of the two time periods, and this could cause the observed transient error.

These two errors are both due to the approximations done to enable the model to be cast in explicit form. For the time scales of importance in this scenario, the discarded pressure waves do not have significant impact on the accuracy of the results.

4.3. Discussion on simulation speed

For the underbalanced drilling connection scenario the simulation time for the full Drift-Flux model was 3630.7 seconds and for the simplified model 661 seconds, when implemented in MATLAB and run on a i7-5500U CPU @ 2.40GHz.

The slow run time of the full DFM is in large part due to the small time step that must be used to accommodate the CFL-condition with the large eigenvalues associated with the propagation of the pressure waves. The full DFM can also be implemented with larger time steps by employing large time step schemes such as proposed by [25], or by treating the pressure wave propagation implicitly through using semi-implicit schemes, see e.g. [9, 14].

The usability of the simplified model becomes more apparent when implemented with a larger grid size. E.g. by setting Δx=20 meters the underbalanced drilling connection scenario runs in 1.56 seconds which corresponds to 2000×real-time, and with some code optimization yet faster run times would be expected. This is a very desirable property when the model has to be run repeatedly as part of a larger numerical algorithm, such as when employed in Model Predictive Control.

5. Summary and conclusions

In this paper we have presented a simplified two-phase flow model obtained by relaxing the distributed pressure dynamics, equivalent to using a quasi-steady momentum balance. The resulting model is a transport equation, with void fraction as the distributed state. The gas travels with an exponentially increasing (for negative pressure gradient), quasi-steady velocity driven by the gas expansion, which is modeled as a source term in the transport equation. The closure relations can be approximated as explicit functions and quadratures of the states and exogenous variables. This enables the implementation of simple, fast and robust two-phase simulators, which is amenable for control and estimation applications where simulation speed and robustness are of importance such as Model Predictive Control [43] and particle filters [38].

To deal with cases where the right boundary condition is specified as a flow rate in place of a pressure, a relation is required to describe the pressure at the boundary. This is done by assuming a lumped pressure for the whole conduit, with dynamics modeled by an ODE coupled with the PDE. The resulting first-order ODE model describing the lumped pressure dynamic can for some applications enable the use of established model-based algorithms in pressure control and estimation problems, where the full DFM is too complicated [1].

Further work on this topic should deal with the following points not yet addressed:

- More elaborate phase behavior models
- Integrate the model with more accurate closure relations for the pressure drop (i.e. the momentum source term) and the slip law.
- Improve the approximations used to make the implementation explicit.
- Handle the phenomena of phase separation in a shut-in scenario.

Acknowledgment

This work was supported by Statoil ASA, the Research Council of Norway (NFR project 210432/E30 Intelligent Drilling) and the Rig Automation and Performance Improvement in Drilling (RAPID) sponsor group (ExxonMobil, Sinopec, Baker Hughes and NOV). The work of the first author was aslo supported by the Research Council of Norway, ConocoPhillips, Det norske oljeselskap, Lundin, Statoil and Wintershall through the research center DrillWell (Drilling and Well Centre for Improved Recovery) at IRIS.

References

[1] Aarsnes, U. J. F., 2016. Modeling of Two-Phase Flow for Estimation and Control of Drilling Operations. Ph.D. thesis, Norwegian University of Science and Technology.

[2] Aarsnes, U. J. F., Ambrus, A., Karimi Vajargah, A., Aamo, O. M., van Oort, E., 2015. A simplified gas-liquid flow model for kick mitigation and control during drilling operations. In: Proc. ASME 2015 Dyn. Syst. Control Conf. Columbus, Ohio, USA.

[3] Aarsnes, U. J. F., Di Meglio, F., Evje, S., Aamo, O. M., Oct. 2014. Control-Oriented Drift-Flux Modeling of Single and Two-Phase Flow for Drilling. In: ASME Dyn. Syst. Control Conf. ASME, San Antonio, Texas, USA, p. V003T37A003.

[4] Aarsnes, U. J. F., Meglio, F. D., Graham, R., Aamo, O. M., 2016. A methodology for classifying operating regimes in underbalanced drilling operations. SPE J.

[5] Ambrus, A., Aarsnes, U. J. F., Karimi Vajargah, A., Akbari, B., van Oort, E., 2015. A Simplified Transient Multi-Phase Model for Automated Well Control Applications. In: Int. Pet. Conf. Doha, Qatar.
[6] Anderson, B. D., Moore, J. B., 1990. Optimal Control Linear quadratic methods. Courier Corporation.
[7] Åström, K. J., Murray, R. M., 2010. Feedback systems: an introduction for scientists and engineers, 2nd Edition. Princeton university press.
[8] Baer, M., Nunziato, J., 1986. A two-phase mixture theory for the deflagration-to-detonation transition (ddt) in reactive granular materials.
[9] Baudin, M., Coquel, F., Tran, Q.-H., Jan. 2005. A Semi-implicit Relaxation Scheme for Modeling Two-Phase Flow in a Pipeline. SIAM J. Sci. Comput. 27 (3), 914–936.
[10] Bendiksen, K. H., Maines, D., Moe, R., Nuland, S., May 1991. The Dynamic Two-Fluid Model OLGA: Theory and Application. SPE Prod. Eng. 6 (02), 171–180.
[11] Bennion, D. B., Thomas, F. B., Bietz, R. F., Bennion, D. W., apr 1996. Underbalanced Drilling, Praises and Perils. In: Permian Basin Oil Gas Recover. Conf. No. December. Society of Petroleum Engineers.
[12] Bhagwat, S. M., Ghajar, A. J., 2014. A flow pattern independent drift flux model based void fraction correlation for a wide range of gas-liquid two phase flow. Int. J. Multiph. Flow 59, 186–205.
[13] Bloemen, H., Belfroid, S., Sturm, W., Verhelst, F., 2006. Soft sensing for gas-lift wells. SPE J. 11 (December), 454–463.
[14] Bruce Stewart, H., Wendroff, B., Dec. 1984. Two-phase flow: Models and methods. J. Comput. Phys. 56 (3), 363–409.
[15] Carlsen, L. A., Nygaard, G., Gravdal, J. E., Nikolaou, M., Schubert, J., Jan. 2008. Performing the Dynamic Shut-In Procedure Because of a Kick Incident When Using Automatic Coordinated Control of Pump Rates and Choke-Valve Opening. In: SPE/IADC Manag. Press. Drill. Underbalanced Oper. Conf. Exhib. Society of Petroleum Engineers.
[16] Choi, J., Pereyra, E., Sarica, C., Lee, H., Jang, I. S., Kang, J., Feb. 2013. Development of a fast transient simulator for gasliquid two-phase flow in pipes. J. Pet. Sci. Eng. 102, 27–35.
[17] Choi, J., Pereyra, E., Sarica, C., Park, C., Kang, J. M., 2012. An efficient drift-flux closure relationship to estimate liquid holdups of gas-liquid two-phase flow in pipes. Energies 5 (12), 5284–5306.
[18] Danielson, T. J., Bansal, K. M., Djoric, B., Duret, E.-D., Johansen, S. T., Hellan, O., 2011. Testing and Qualification of a New Multiphase Flow Simulator. In: Offshore Technol. Conf. Offshore Technology Conference, pp. 1–16.
[19] Di Meglio, F., 2011. Dynamics and control of slugging in oil production. Phd thesis, ParisTech.
[20] Di Meglio, F., Kaasa, G.-o., Petit, N., Alstad, V., Jun. 2010. Model-based control of slugging flow: An experimental case study. In: Proc. 2010 Am. Control Conf. IEEE, pp. 2995–3002.
[21] Di Meglio, F., Kaasa, G.-O., Petit, N., Alstad, V., Dec. 2010. Reproducing slugging oscillations of a real oil well. In: 49th IEEE Conf. Decis. Control. IEEE, pp. 4473–4479.
[22] Eikrem, G. O., Aamo, O. M., Foss, B., May 2008. On Instability in Gas Lift Wells and Schemes for Stabilization by Automatic Control.
[23] Esmaeil, J., Skogestad, S., Aug. 2011. Simplified Dynamical Models for Control of Severe Slugging in Multiphase Risers. In: Sergio, B. (Ed.), Proc. 18th IFAC World Congr. 2011. Milano, Italy, pp. 1634–1639.
[24] Evje, S., Fjelde, K. K., Jan. 2002. Hybrid Flux-Splitting Schemes for a Two-Phase Flow Model. J. Comput. Phys. 175 (2), 674–701.
[25] Evje, S., Flåtten, T., Oct. 2006. CFL-Violating Numerical Schemes for a Two-Fluid Model. J. Sci. Comput. 29 (1), 83–114.
[26] Evje, S., Wen, H., apr 2013. Weak solutions of a gas-liquid drift-flux model with general slip law for wellbore operations. Discret. Contin. Dyn. Syst. 33 (10), 4497–4530.
[27] Evje, S., Wen, H., 2015. Global Solutions of a Viscous Gas-Liquid Model with Unequal Fluid Velocities in a Closed Conduit. SIAM J. Math. Anal. 47 (1), 381–406.
[28] Fjelde, K. K., Rommetveit, R., Merlo, A., Lage, A. C., Apr. 2003. Improvements in Dynamic Modeling of Underbalanced Drilling. In: IADC/SPE Underbalanced Technol. Conf. Exhib. No. 3. Society of Petroleum Engineers, Houston, Texas.
[29] Flåtten, T., Lund, H., Dec. 2011. Relaxation two-phase flow models and the subcharacteristic condition. Math. Model. Methods Appl. Sci. 21 (12), 2379–2407.
[30] Gavrilyuk, S., Fabre, J., 1996. Lagrangian coordinates for a drift-flux model of a gas-liquid mixture. Int. J. Multiph. flow, 453–460.
[31] Godhavn, J.-M., Aug. 2011. Drilling Seeking Automatic Control Solutions. In: Sergio, B. (Ed.), 18th IFAC World Congr. Milano. Milano, Italy, pp. 10842–10850.
[32] Hauge, E., Godhavn, J., Molde, D., Cohen, J., Stave, R., Toftevaag, K., 2015. Analysis of Field Trial Well Control Results with a Dual Gradient Drilling System. In: Offshore Technol. Conf. Offshore Technology Conference.
[33] Ishii, M., Oct. 1977. One-dimensional drift-flux model and constitutive equations for relative motion between phases in various two-phase flow regimes. Tech. rep., Argonne National Laboratory (ANL), Argonne, IL (United States).
[34] Kaasa, G.-O., Stamnes, Ø. N., Imsland, L. S., Aamo, O. M., 2012. Simplified hydraulics model used for intelligent estimation of downhole pressure for a managed-pressure-drilling control system. SPE Drill. Complet. 27 (March), 127—-138.
[35] Lage, A., Time, R., Oct. 2000. Mechanistic Model for Upward Two-Phase Flow in Annuli. Proc. SPE Annu. Tech. Conf. Exhib. (1), 1–11.
[36] Linga, G., 2015. A Hierarchy of Non-Equilibrium Two-Fluid Models. SIAM J. Appl. Math. (Submitted).
[37] Lorentzen, R. J., Fjelde, K. K., Jul. 2005. Use of slopelimiter techniques in traditional numerical methods for multi-phase flow in pipelines and wells. Int. J. Numer. Methods Fluids 48 (7), 723–745.
[38] Lorentzen, R. J., Stordal, A., Nævdal, G., Karlsen, H. A., Skaug, H. J., Feb. 2014. Estimation of Production Rates With Transient Well-Flow Modeling and the Auxiliary Particle Filter. SPE J. 19 (01), 172–180.
[39] Masella, J., Tran, Q., Ferre, D., Pauchon, C., Aug. 1998. Transient simulation of two-phase flows in pipes. Int. J. Multiph. Flow 24 (5), 739–755.
[40] Minami, K., Shoham, O., sep 1994. Transient two-phase flow behavior in pipelines-experiment and modeling. Int. J. Multiph. Flow 20 (4), 739–752.
[41] Nygaard, G. H., Vefring, E. H., Mylvaganam, S., Fjelde, K. K., Apr. 2004. Underbalanced Drilling: Improving Pipe Connection Procedures Using Automatic Control. In: SPE Annu. Tech. Conf. Exhib. Society of Petroleum Engineers.
[42] Pauchon, C., Dhulesia, H., 1994. TACITE: A Transient Tool for Multiphase Pipeline and Well Simulation. In: SPE Annu. Tech. Conf. Exhib. No. 58. Society of Petroleum Engineers, pp. 62–77.

[43] Pedersen, T., Godhavn, J.-M., 2013. Model Predictive Control of Flow and Pressure in Underbalanced Drilling. In: 10th IFAC Int. Symp. Dyn. Control Process Syst. pp. 307–312.
[44] Pedersen, T., Godhavn, J.-M., Schubert, J., 2015. Supervisory control for underbalanced drilling operations. IFAC-PapersOnLine 48 (6), 120–127.
[45] Shayegi, S., Kabir, C. S., If, F., Christensen, S., Ken, K., Casasus-Bribian, J., Hasan, A. K., Moos, D., mar 2012. Reservoir Characterization Begins at First Contact With the Drill Bit. SPE Drill. Complet. 27 (01), 11–21.
[46] Shi, H., Holmes, J., Durlofsky, L., Aziz, K., Diaz, L., Alkaya, B., Oddie, G., Mar. 2005. Drift-Flux Modeling of Two-Phase Flow in Wellbores. SPE J. 10 (1), 24–33.
[47] Suryanarayana, P., Vaidya, R. N., Wind, J., 2007. Use of a New Rate-Integral Productivity Index in Interpretation of Underbalanced Drilling Data for Reservoir Characterization. In: Prod. Oper. Symp. Society of Petroleum Engineers.
[48] Taitel, Y., Barnea, D., jun 1997. Simplified transient simulation of two phase flow using quasi-equilibrium momentum balances. Int. J. Multiph. Flow 23 (3), 493–501.
[49] Taitel, Y., Shoham, O., Brill, J., 1989. Simplified transient solution and simulation of two-phase flow in pipelines. Chem. Eng. Sci. 44 (6), 1353–1359.
[50] Teixeira, B. O., Castro, W. S., Teixeira, A. F., Aguirre, L. a., Jan. 2014. Data-driven soft sensor of downhole pressure for a gas-lift oil well. Control Eng. Pract. 22, 34–43.
[51] Zuber, N., Findlay, J. A., 1965. Average Volumetric Concentration in Two-Phase Flow Systems. J. Heat Transfer 87 (4), 453.